<u>Supplementary Information</u>

The 3D structure of lipidic fibrils of α-synuclein

Benedikt Frieg[1*], Leif Antonschmidt[2*], Christian Dienemann[3], James A. Geraets[1], Eszter E. Najbauer[2], Dirk Matthes[4], Bert L. de Groot[4], Loren B. Andreas[2], Stefan Becker[2], Christian Griesinger[2,5], and Gunnar F. Schröder[1,6]

[1] Institute of Biological Information Processing (IBI-7: Structural Biochemistry) and JuStruct: Jülich Center for Structural Biology, Forschungszentrum Jülich; Jülich, Germany.

[2] Department of NMR-Based Structural Biology, Max Planck Institute for Multidisciplinary Sciences; Göttingen, Germany.

[3] Department of Molecular Biology, Max Planck Institute for Multidisciplinary Sciences; Göttingen, Germany.

[4] Department of Theoretical and Computational Biophysics, Max Planck Institute for Multidisciplinary Sciences; Göttingen, Germany.

[5] Cluster of Excellence "Multiscale Bioimaging: From Molecular Machines to Networks of Excitable Cells" (MBExC), University of Göttingen; Göttingen, Germany.

[6] Physics Department, Heinrich Heine University Düsseldorf; Düsseldorf, Germany.

*These authors contributed equally to this work.
Correspondence and requests for materials should be addressed to Gunnar F. Schröder (gu.schroeder@fz-juelich.de) and Christian Griesinger (cigr@mpinat.mpg.de).

Supplementary figures and legends
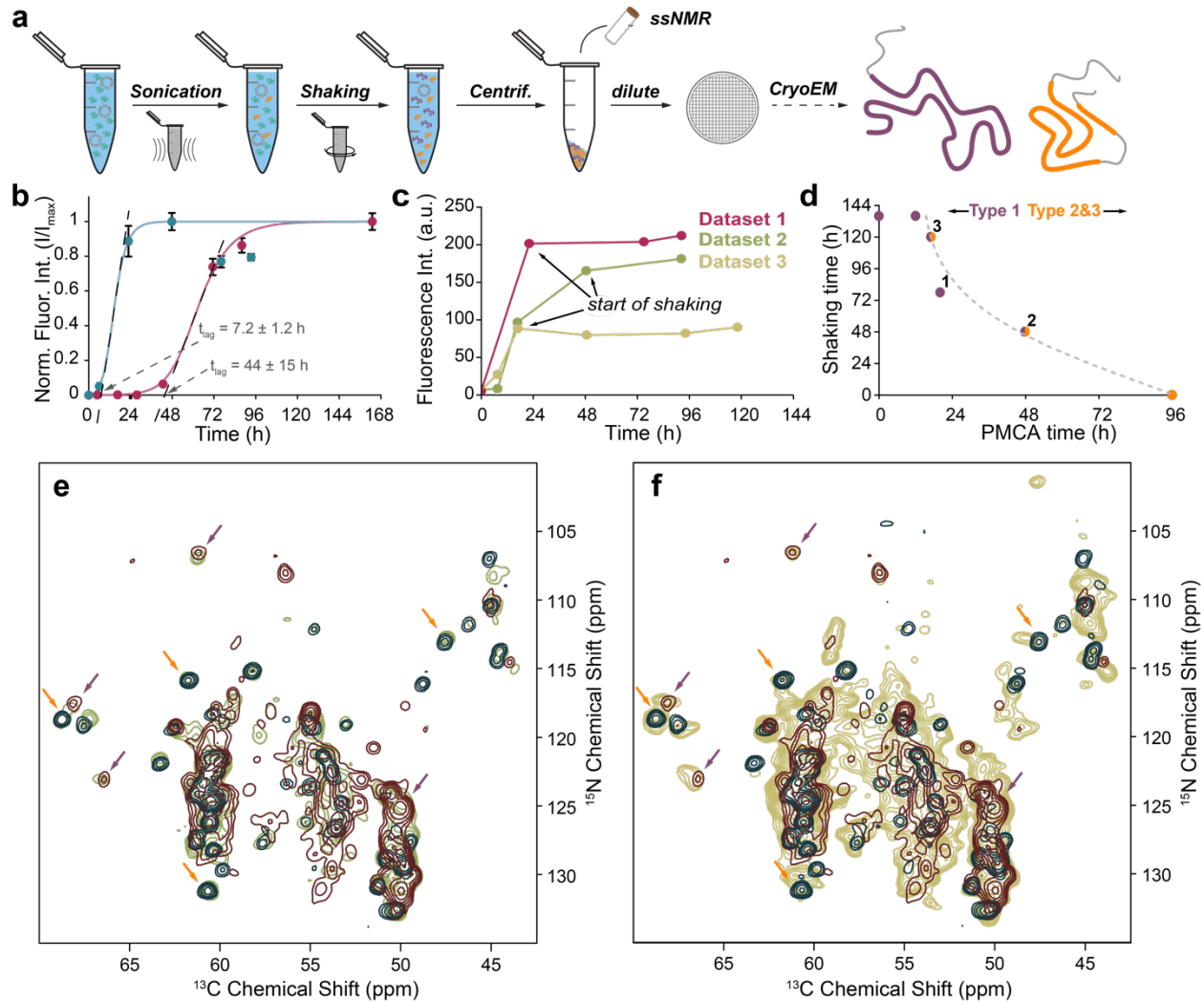
Supplementary Figure 1 | Preparation and characterization of fibril samples.
**a**, Workflow schematic for preparation of αSyn fibrils in this study. **b,** Representative curves of normalized ThT fluorescence (I/I_{max}) following the aggregation kinetics of αSyn in the presence (blue) and absence (magenta) of vesicles of POPA and POPC (1:1) under PMCA conditions. Curves were obtained by fitting the data to an unseeded secondary nucleation model using Amylofit[1] (www.amylofit.ch.cam.ac.uk/). Data are presented as mean values +/- SD averaged over two scans. Lag-times t_{lag} were determined as the intersection of the x-axis and a linear function fitted to the steepest part of the curve **c,** ThT fluorescence data of individual samples analyzed by cryo-EM. **d,** Correlation plot of times spent under different agitation conditions. Points are color coded by the dominant fibril types. Characterization of type L1 (purple) and type L2 & L3 (orange) was done by ssNMR (fibril subtypes were indistinguishable) and in labelled cases by Cryo-EM (datasets 1-3). **e,** (H)CANH spectra of αSyn fibrils used for dataset 1 acquired at 800 MHz with 55 kHz MAS (green) and **f,** (H)NCA of αS fibrils used for dataset 2 acquired at 850 MHz with 17 kHz MAS (yellow) compared to spectra of fibrils prepared under purely PMCA (blue, 950 MHz, 100 kHz MAS) and shaking conditions (red, 1200 MHz, 55 kHz MAS). Arrows indicate characteristic peaks originating from either L1 (purple) or L2/L3 fibrils (orange), showing that in

either sample a mixture of both fibril types is present. Spectra of fibrils prepared under PMCA conditions (blue) are reproduced from ref.[2].
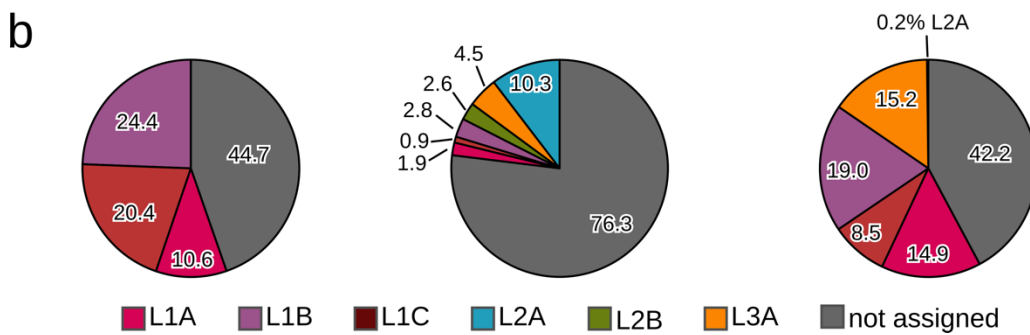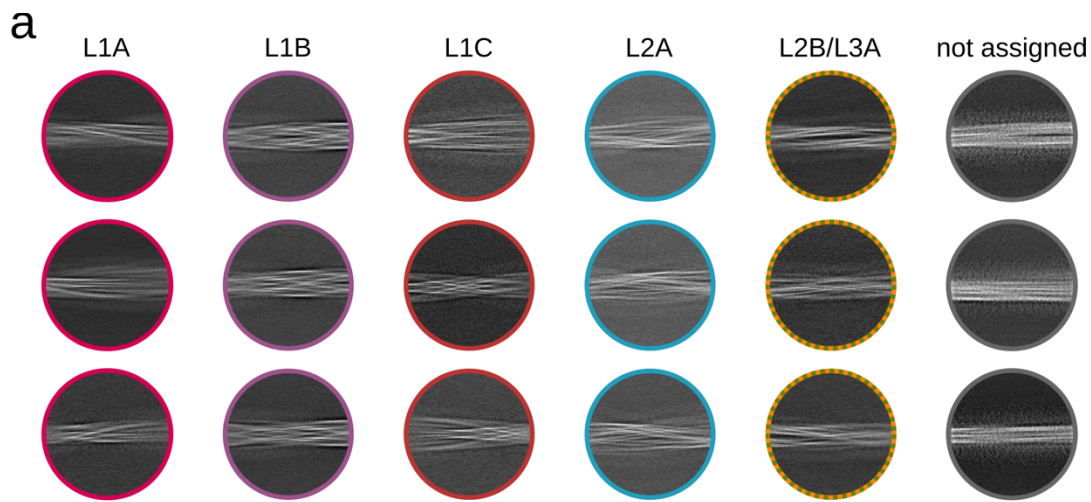

Supplementary Figure 2 | Distribution of lipid-induced αSyn fibrils.
a, Representative 2D class averages for all lipid-induced αSyn fibrils and segments that could not be assigned to any of the polymorphs after 2D classification, due to the lack of well-defined and clear filament features. Instead, the unassigned classes are not sharp and partially very fuzzy at the fibril surface. **b**, Pie charts visualizing the relative population (labels in %) of each lipid-induced αSyn fibril polymorphs in dataset 01 (left) 02, (middle), and 03 (right).
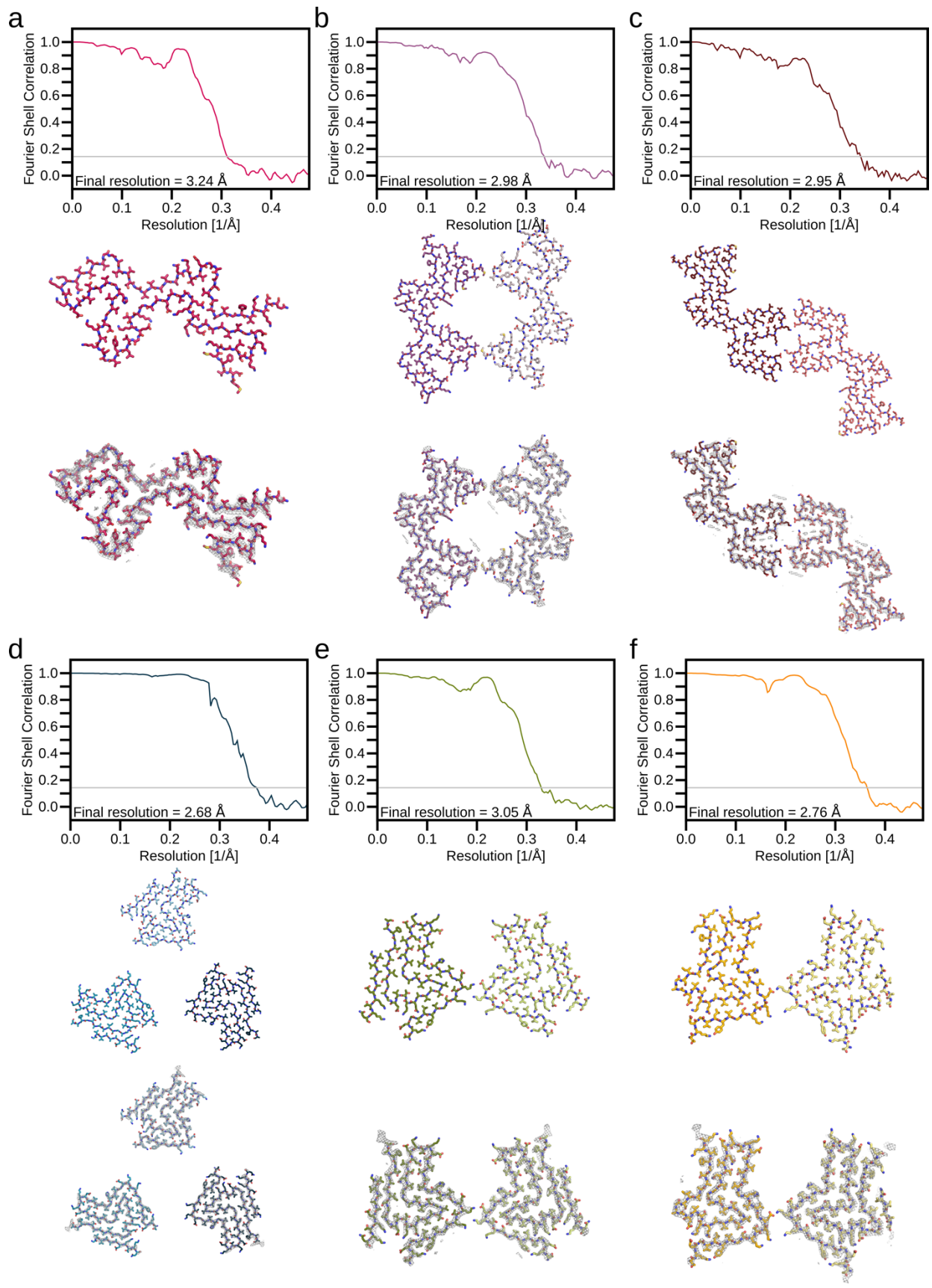
Supplementary Figure 3 | Fourier shell correlation curves, final cryo-EM density maps, and atomic model of the lipidic αSyn fibrils.

55   Masked-corrected (z-percentage is 0.1) Fourier shell correlation (FSC) curves (top panels), the atomic model (middle panels), and a superposition of the atomic model and the central slice of the density map with a width of 10.5 Å (10 pixel, 1.05 Å/pixel; gray isomesh) (lower panels) for L1A (**a**), L1B (**b**), L1C (**c**), L2A (**d**), L2B (**e**), and L3A (**f**). The final resolution is shown in the plot and was estimated from the value of the FSC curve for two separately refined masked half-maps at

60   0.143 (gray line).
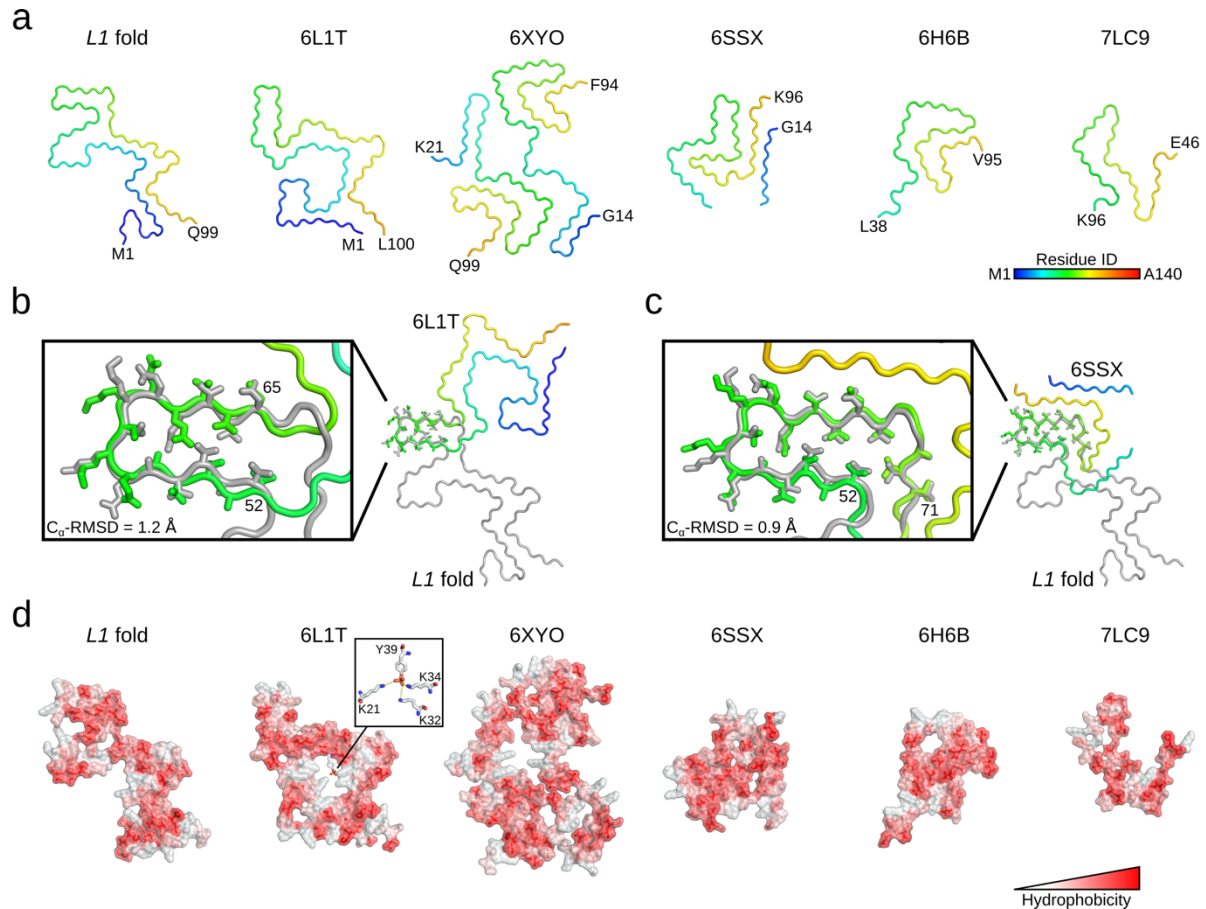
Supplementary Figure 4 | Comparison of the lipidic *L1* fold and known structures.
a: Backbone traces of previously resolved αSyn structures, with residues colored according to the rainbow pallet in the lower right corner. The four-letter PDB-ID is reported with the structures (6L1T: protofilament fold of Y39 phosphorylated αSyn[3]; 6XYO: fold of MSA Type I filaments[4]; 6SSX: protofilament fold of polymorph 2[5]; 6H6B: protofilament fold of polymorph 1[6]; 7LC9: protofilament fold of the structure of the N-terminal αSyn truncation 41-140[7]). The labels depict the N- and C-terminal residues. **b**, **c**: Superposition of the lipidic L1 fold (gray) with PDB-ID 6L1T (**b**) and PDB-ID 6SSX (**c**). The residues considered for the superposition are shown as sticks in the close-up view, along with the Cα-RMSD of the superposition. **d**: Stick-surface models from (**a**), but now colored according to the Eisenberg hydrophobicity scale[8]. For PDB-ID 6L1T, the close-up view shows interactions mediated by the phosphorylated Y39, which form the core of the protofilament fold.

a

b
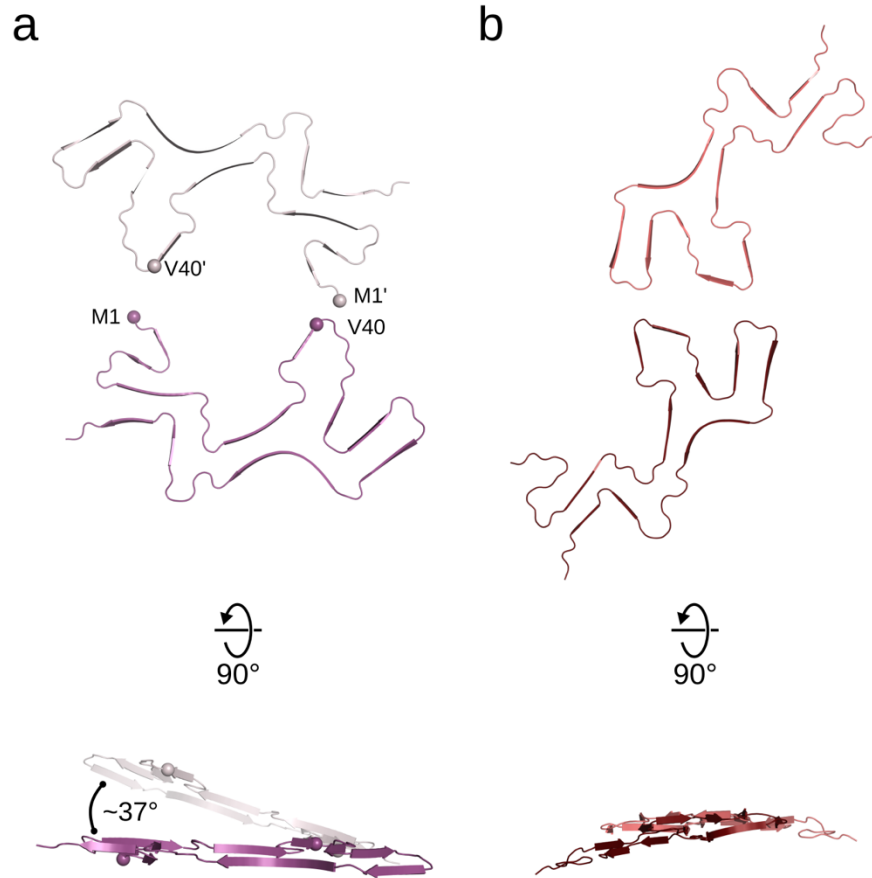
Supplementary Figure 5 | The tilting of protofilaments in the *L1B* fibril.
Two central protein chains extracted from the L1B (**a**) and L1C (**b**) αSyn fibril models in top and side-view. To estimate the tilt angle between the protofilaments in L1B, we measured the dihedral angle described by the Cα atoms of M1-V40-M1'-V40' of two opposite protein chains.
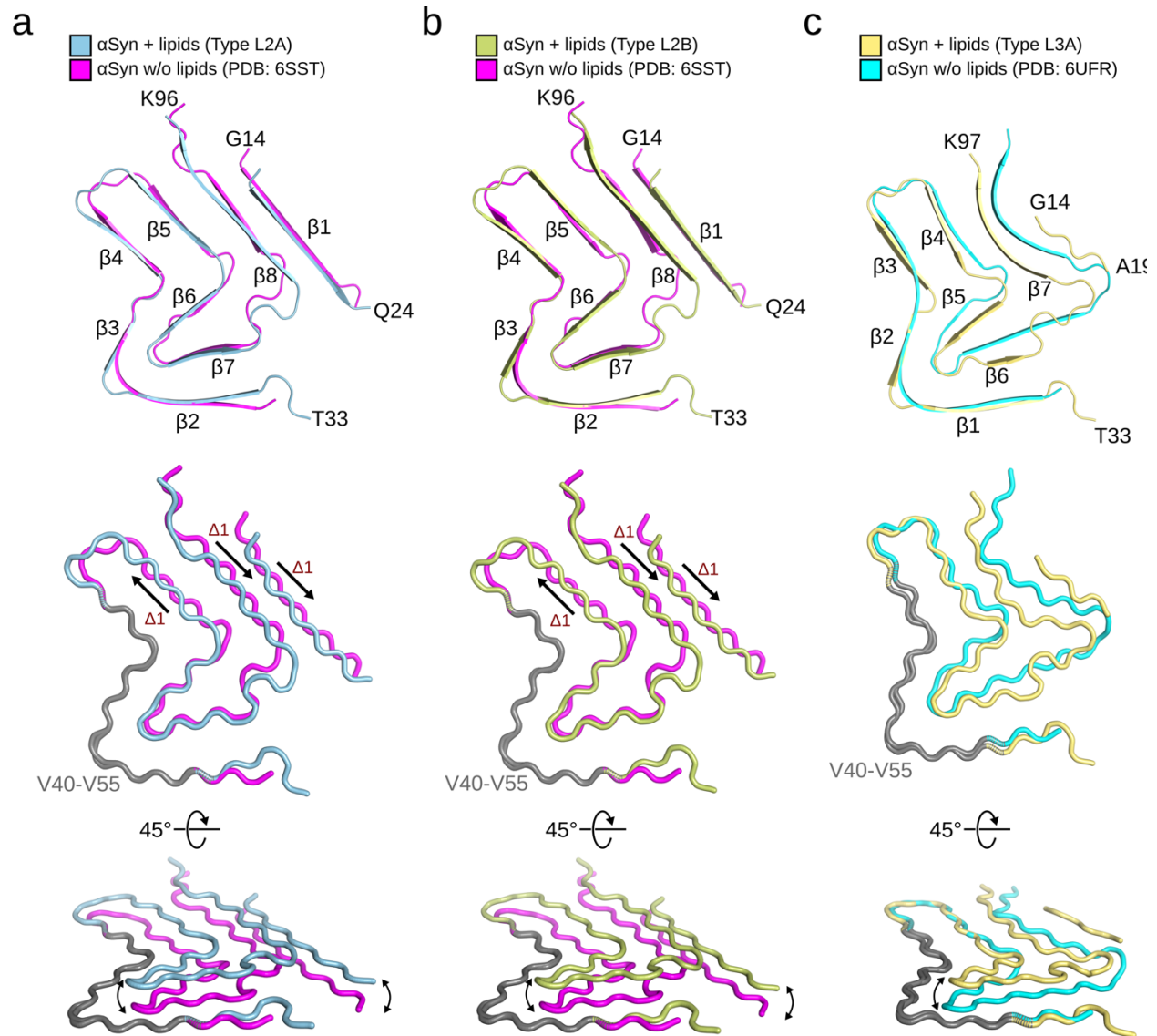
Supplementary Figure 6 | Comparison between *L2* and *L3* fibrils and known structures.
Superposition of a single protein chain of (**a**) L2A αSyn onto in vitro aggregated wild type αSyn (PDB: 6SST [5]; Cα RMSD = 2.9 Å), (**b**) L2B αSyn onto in vitro aggregated wild type αSyn (PDB: 6SST [5]; Cα RMSD = 3.0 Å), and (**C**) L3A αSyn onto in vitro aggregated E46K αSyn (PDB: 6UFR [9]; Cα RMSD = 3.0 Å). Termini and β-strands are labeled. The middle panel visualizes the relative shift of β1, β5, and β8 introduced by the presence of lipids, after superimposing V40 to V55 (gray). The lower panel indicates the out-of-plane shift induced by the presence of lipids, as shown on a single chain.

a

90° 90° 90° 90°

90° 90° 90° 90°

Supplementary Figure 7 (consecutive)

9

b
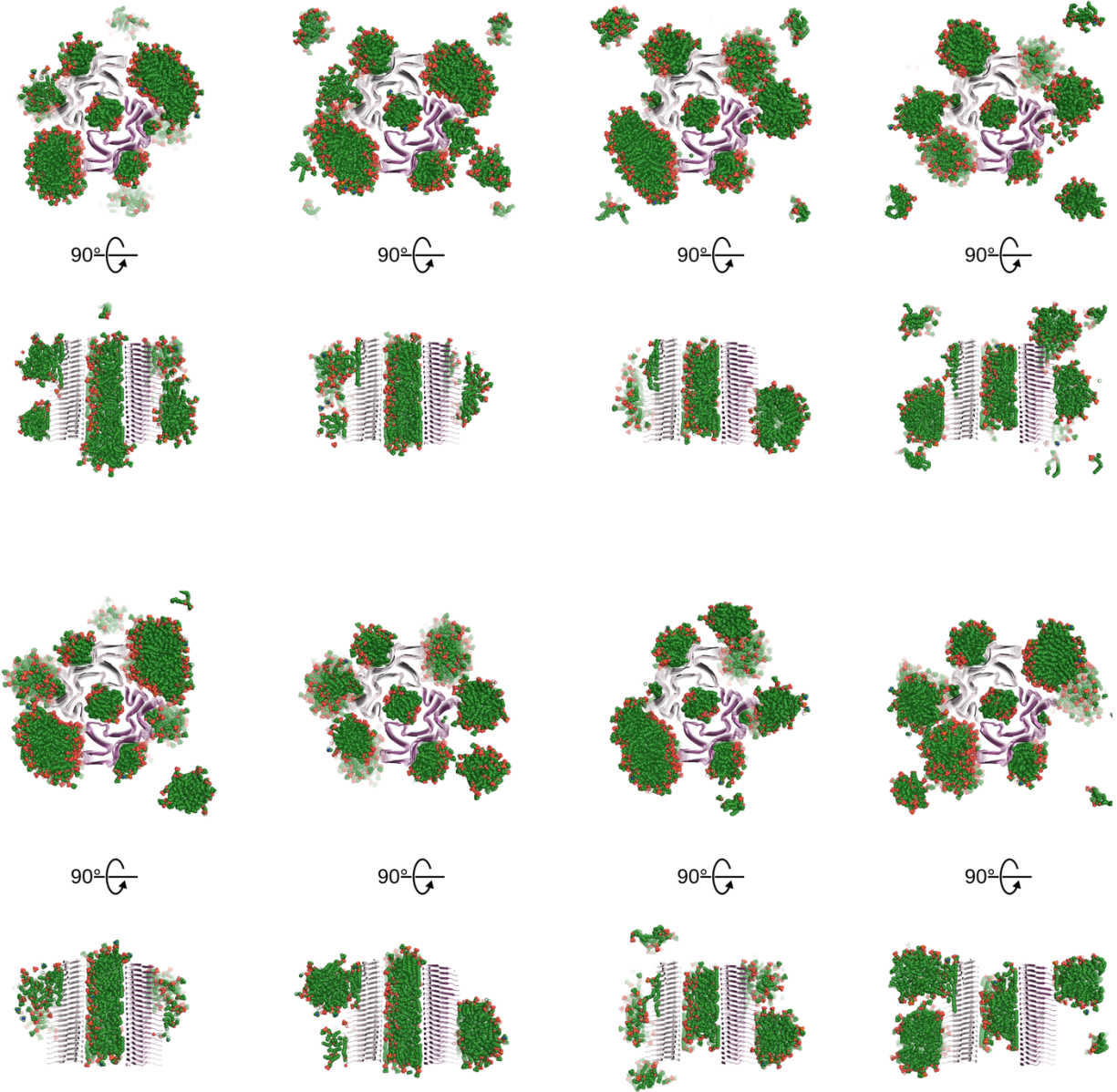
Supplementary Figure 7 (consecutive)

c
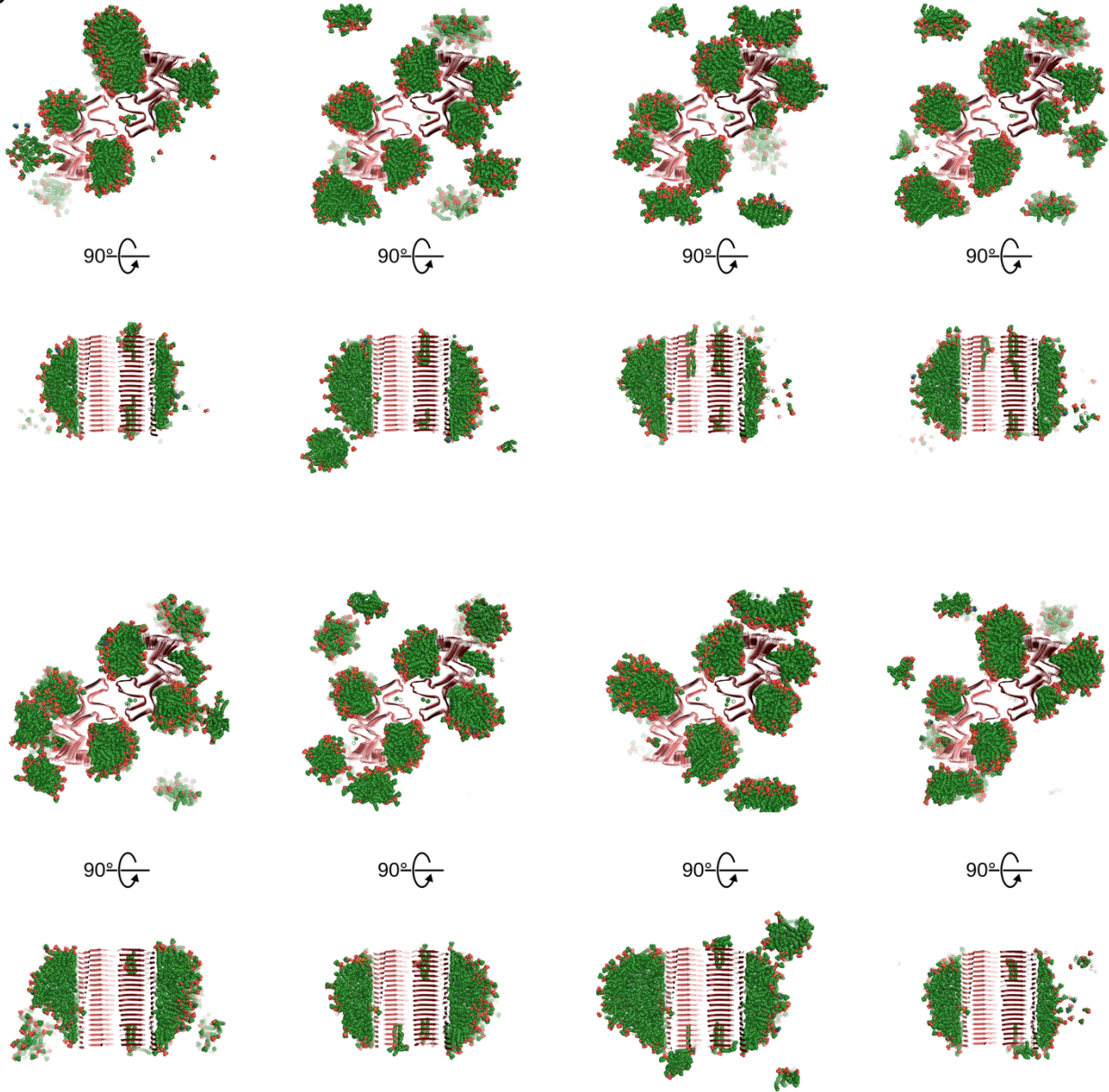
Supplementary Figure 7 (consecutive)

d
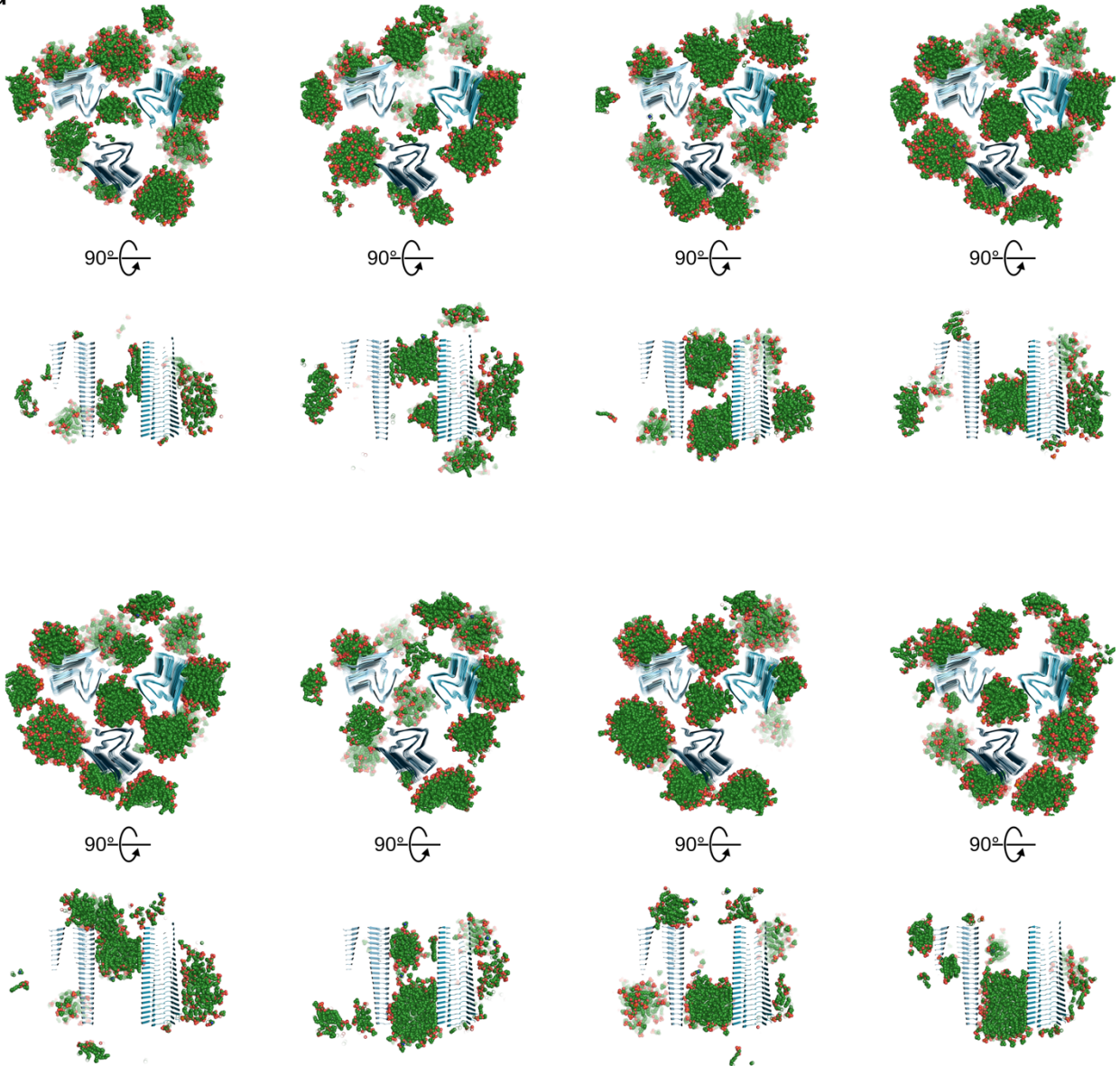
105

Supplementary Figure 7 (consecutive)

e

Supplementary Figure 7 (consecutive)

f
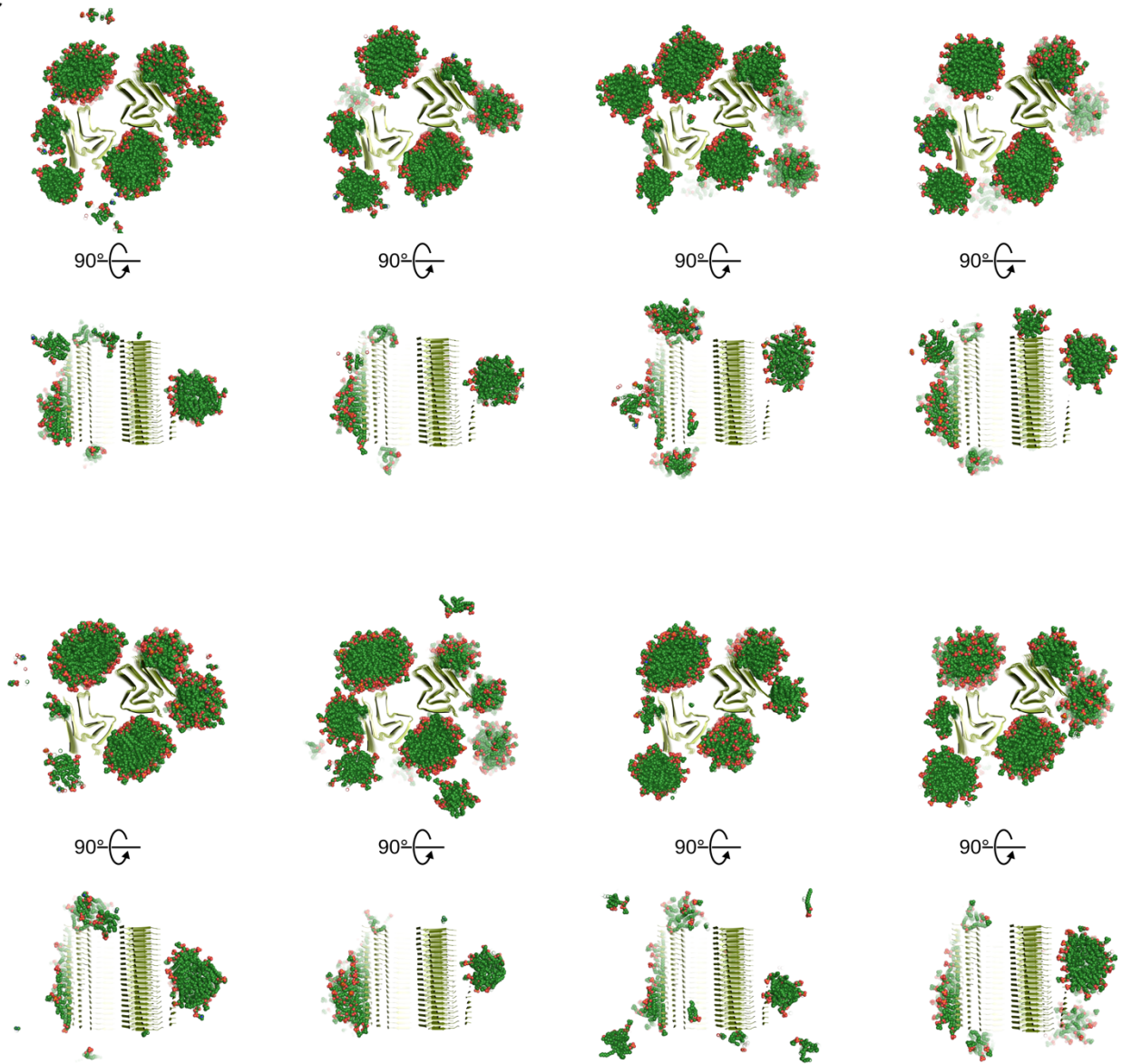
Supplementary Figure 7 | Molecular dynamics simulations of the unbiased lipid diffusion. Cross-section through the conformations after eight 1 µs MD simulations of unbiased lipid diffusion in the presence of the lipidic for L1A (**a**), L1B (**b**), L1C (**c**), L2A (**d**), L2B (**e**), or L3A (**f**) fibril, viewed from two perspectives. The fibril is shown as cartoon, the lipids as green spheres.
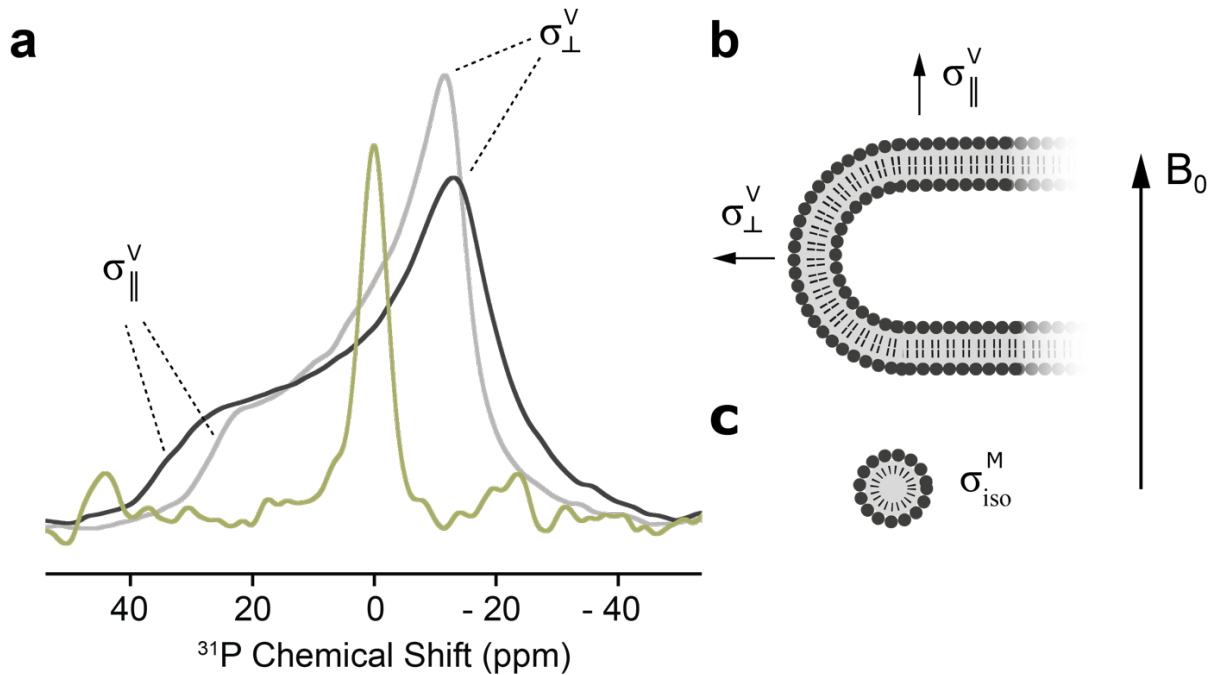
Supplementary Figure 8 | The conversion of the SUVs to small lipid aggregates during fibril preparation.

a, ^{1}H decoupled static ^{31}P ssNMR spectra of vesicles of POPA and POPC (1:1) at 280 K (black) and 310 K (grey) compared to the spectrum of lipidic αSyn fibrils at 280 K (green, same sample as dataset 2). Spectra of vesicles show a characteristic powder pattern due to chemical shift anisotropy (CSA) after uniaxial diffusion of the lipid molecule about its own long axis. Lateral diffusion of lipid molecules does not result in significant reorientation, consistent with lipid bilayer structures of low curvature (**b**). Lipids bound to αSyn fibrils show a single sharp line, indicating that CSA is averaged via isotropic reorientation of lipid headgroup moieties, consistent with the presence of high-curvature lipid aggregates, such as micelles (**c**). This behavior cannot be explained by a change of the lipid transition temperature and a resulting increase in mobility, since even at higher temperatures the vesicle spectra do not show a comparably sharp line.
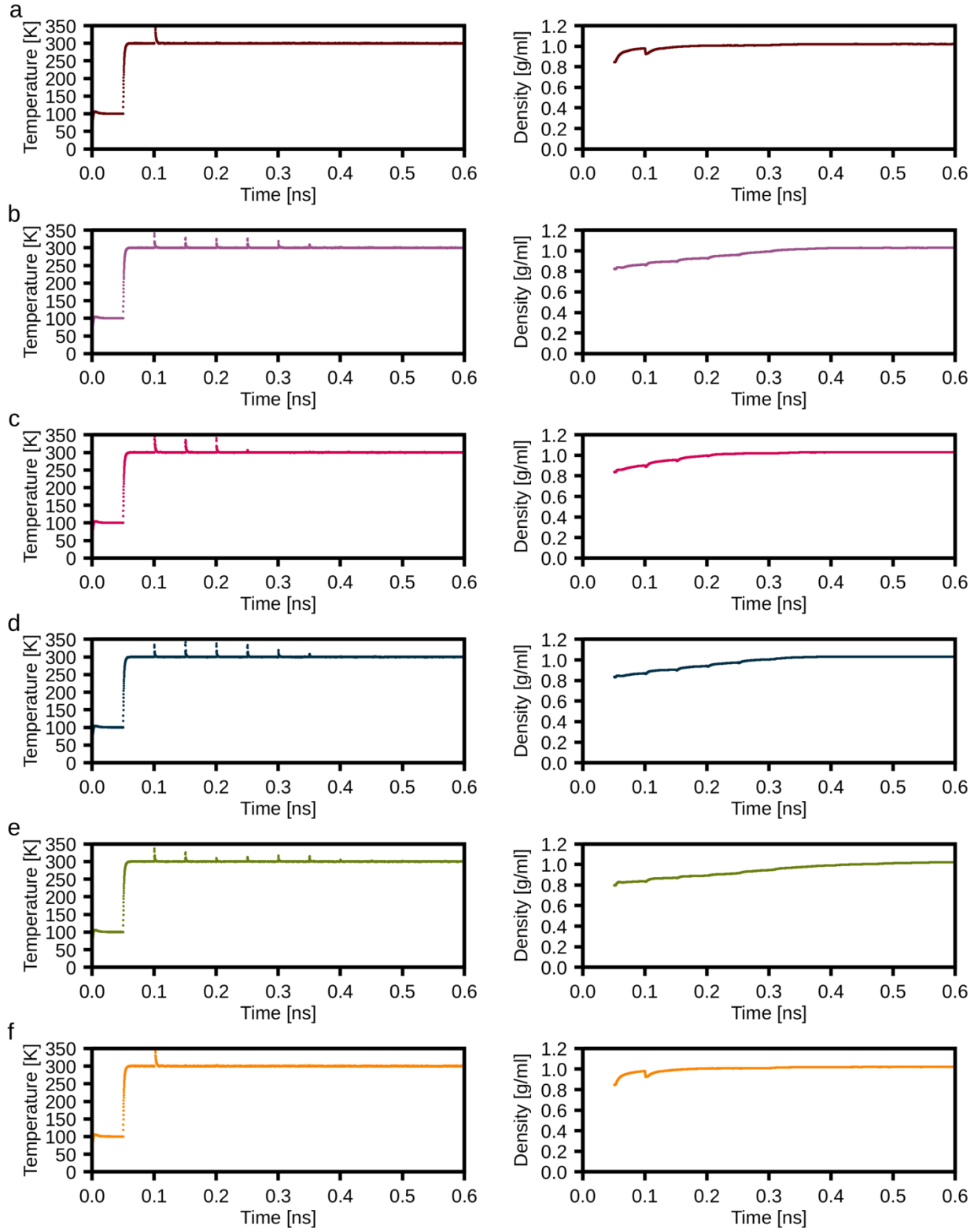
Supplementary Figure 9 | Thermalization and density adaptation data of molecular dynamics simulations.

Time series of the temperature (left panels) and density (right panels) over 0.6 ns of MD simulations for L1A (**a**), L1B (**b**), L1C (**c**), L2A (**d**), L2B (**e**), and L3A (**f**). The MD simulation procedure[10] started by heating the systems from 0 K to 100 K in a canonical (NVT) MD simulation of 50 ps length. Afterward, the temperature was raised from 100 K to 300 K during 50 ps of isobaric-isothermal (NPT) MD. Subsequently, the density was gently adjusted to 1 g/ml during 200 ps of NPT-MD. During the heating and density adaptation steps, positional restraints of 1 kcal·mol^{-1}·Å^{-2} were applied to all backbone and lipidic phosphate atoms. These harmonic positional restraints were removed from the lipidic phosphate atoms by gradually decreasing the force constant from 1 to 0 kcal·mol^{-1}·Å^{-2} in six NPT-MD runs of 50 ps length. From here, we (re-)started eight independent NPT production simulations at 300 K and 1 bar for 1 μs each, in that new velocities were assigned from Maxwell-Boltzmann distribution. Importantly, we restrained the backbone to the initial atomic coordinates throughout production simulations while all other atoms were allowed to move freely.

Supplementary Figure 10 | Structural analyses of fibrils during MD simulations without positional restraints and without lipids.

The plots show the backbone root mean square deviations (RMSD) throughout four replica (colored differently) MD simulations of 1 µs length relative to the starting structures. In contrast to the simulations used to calculate the distribution of phospholipids (**Figure 3**), here we performed simulations without any positional restraints and in the absence of phospholipids, leading to increased RMSD values, which indicates pronounced structural deviation from the starting structure. In the case of L2A, we only simulated one protofilament, since the three protofilaments were not in contact at all.
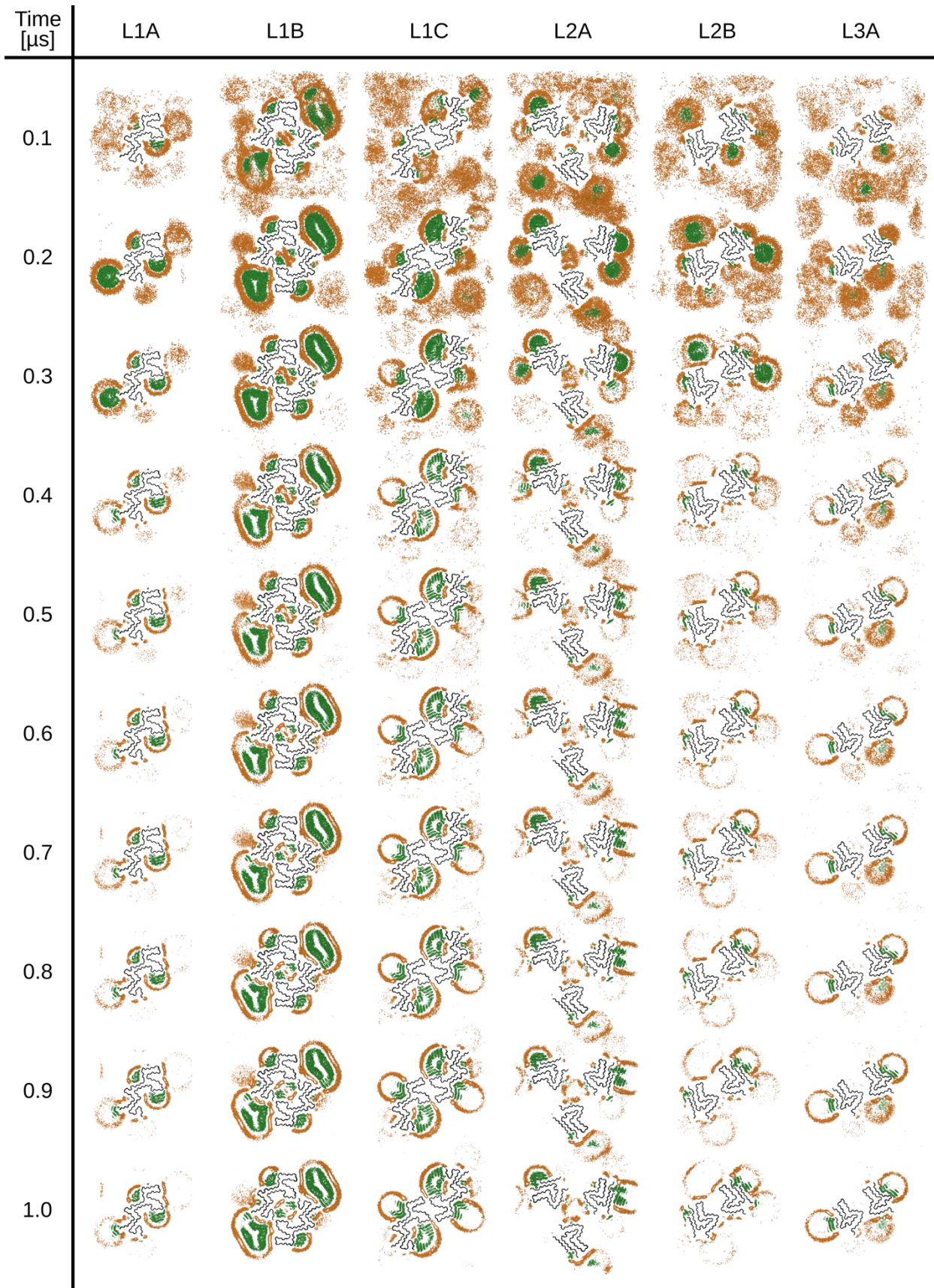
Supplementary Figure 11 | Progression of lipid density grids during single replica simulations of all six fibrils.

160

Cross-section views (the central 15 Å of the fibrils) showing grids indicating the probability density of the lipid acyl chain (dark green) and lipidic phosphate atoms (orange) with increasing simulation time (in 0.1 µs intervals). The fibrils' backbones are shown as black ribbons.

Supplementary Table 1 | Cryo-EM structure determination statistics.

Lipid-induced PM	L1A	L1B	L1C	L2A	L2B	L3A
Data collection						
Microscope	Titan Krios G2	Titan Krios G2			Titan Krios G2	
Voltage [keV]	300	300			300	
Detector	K3	K3			K3	
Magnification	81,000	81,000			81,000	
Pixel size [Å]	1.05	1.05			1.05	
Defocus range [μm]	-0.5 to -2.0	-0.7 to -2.0			-0.5 to -2.0	
Exposure time [s/frame]	2.997	2.997			2.997	
Number of frames	40	50			40	
Total dose [e$^-$/Å^2]	42.72 (1.07 e$^-$/Å^2/frame)	50.83 (1.02 e$^-$/Å^2/frame)			42.72 (1.07 e$^-$/Å^2/frame)	
Reconstruction						
Micrographs	4,589	4,324			4,542	
Box width [pixels]	250	250			250	
Inter-box distance [pixels]	14	14			14	
Picked segments (no.)	585,342	504,236			1,223,706	
	L1A	L1B	L1C	L2A	L2B	L3A
PDB-ID	8ADU	8ADV	8ADW	8A4L	8ADS	8AEX
EMDB-ID	15370	15371	15372	15148	15369	15388
Final segments [no.]	13,641	19,108	25,817	46,003	20,388	46,882
Final resolution [Å] (FSC=0.143)	3.24	2.98	2.95	2.68	3.05	2.76
Applied map sharpening B-factor [Å^2]	-85.24	-83.67	-87.28	-98.95	-78.72	-85.99
Symmetry imposed	C1	C1	C2	C3	C1	C1
Helical rise [Å]	4.69	2.37	4.69	4.68	4.69	4.72
Helical twist [°]	-0.96	179.49	-0.72	-0.75	-0.82	-0.95

Supplementary Table 2 | Model building statistics.

Lipid-induced PM	L1A	L1B	L1C	L2A	L2B	L3A
Initial model [PDB code]	de novo	de novo	de novo	6SST	6SST	6UFR
Model composition						
Chains	5	10	10	15	10	10
Non-hydrogen atoms	3,460	6,920	6,920	7,755	5,170	4,665
Protein residues	495	990	990	1,125	750	680
RMS deviations						
Bond lengths [Å]	< 0.01	< 0.01	0.01	< 0.01	< 0.01	0.01
Bond angles [°]	0.82	0.64	1.5	0.65	0.42	1.16
Validation						
MolProbity score	2.39	2.37	2.95	1.53	1.32	2.49
Clashscore	20.22	16.36	8.01	10.11	5.84	12.49
Ramachandran plot						
Outliers [%]	0	0	0	0	0	0
Allowed [%]	11.34	9.28	7.73	0	0	8.46
Favored [%]	88.66	90.72	92.27	100	100	91.54

5

Supplementary Movie S1. Lipid binding to the *L1B* αSyn fibril.

The movie shows the first 100 ns of a representative trajectory of randomly placed phospholipids (1:1 mixture of POPC/POPA) binding to the *L1B* αSyn fibril. The lipids are shown as green-sphere model, and the αSyn fibril as cartoon, with both protofilaments colored differently.

Supplementary References

1. Meisl, G. et al. Molecular mechanisms of protein aggregation from global fitting of kinetic models. *Nat. Protoc.* **11**, 252-272 (2016).
2. Antonschmidt, L. et al. Insights into the molecular mechanism of amyloid filament formation: Segmental folding of alpha-synuclein on lipid membranes. *Sci. Adv.* **7**, eabg2174 (2021).
3. Zhao, K. et al. Parkinson's disease-related phosphorylation at Tyr39 rearranges alpha-synuclein amyloid fibril structure revealed by cryo-EM. *Proc. Natl. Acad. Sci. U. S. A.* **117**, 20305-20315 (2020).
4. Schweighauser, M. et al. Structures of alpha-synuclein filaments from multiple system atrophy. *Nature* **585**, 464-469 (2020).
5. Guerrero-Ferreira, R. et al. Two new polymorphic structures of human full-length alpha-synuclein fibrils solved by cryo-electron microscopy. *Elife* **8**, e48907 (2019).
6. Guerrero-Ferreira, R. et al. Cryo-EM structure of alpha-synuclein fibrils. *Elife* **7**(2018).
7. McGlinchey, R.P., Ni, X.D., Shadish, J.A., Jiang, J.S. & Lee, J.C. The N terminus of alpha-synuclein dictates fibril formation. *Proc. Natl. Acad. Sci. U. S. A.* **118**(2021).
8. Eisenberg, D., Schwarz, E., Komaromy, M. & Wall, R. Analysis of membrane and surface protein sequences with the hydrophobic moment plot. *J. Mol. Biol.* **179**, 125-142 (1984).
9. Boyer, D.R. et al. The alpha-synuclein hereditary mutation E46K unlocks a more stable, pathogenic fibril structure. *Proc. Natl. Acad. Sci. U. S. A.* **117**, 3592-3602 (2020).
10. Frieg, B. et al. Molecular mechanisms of glutamine synthetase mutations that lead to clinically relevant pathologies. *PLoS Comput. Biol.* **12**, e1004693 (2016).

nature portfolio

Peer Review File

REVIEWER COMMENTS

Reviewer #1 (Remarks to the Author):

Frieg et al. present cryo-EM analysis of phospholipid-induced α-synuclein (lipid-α-syn) fibril structures, and reveal the structural basis of the interaction between lipid and α-syn in fibrillar form from the additional cryo-EM densities of on lipid-α-syn fibril together with MD simulations and ssNMR data. The authors determine six lipid-α-syn fibril complex structures. Interestingly, three L1 fibrils possess a novel protofilament fold type, which expands the structural knowledge on the structural polymorphism of α-syn amyloid fibril. L2 and L3 feature previously knownα-syn fold in fibril structures, but with distinct protofilamental arrangement. Moreover, the MD simulations of lipid diffusion in the presence ofα-syn fibril structure suggest a micelle-like lipid arrangements at the fibril surface and the central cavity, which matches the cryo-EM densities well. By further performing ssNMR, the authors assign the fibril-lipid interactions for each fibril polymorph. Both lipid and α-syn fibrils are enriched in Lewy bodies in the patients' brains of Parkinson's disease. Elucidating lipid-α-syn fibril interaction is important to understanding the molecular basis of α-syn pathological aggregation and Lewy body formation in PD. Thus, this work is timely and important to the field. Overall, the results are well presented in a logic format, and the complex structural models are cross-validated by different biophysical and computational methods. To strengthen this work, the authors may need to address my concerns listed below.

Major concerns:
1. The authors perform MD simulations for phospholipid diffusion and show probability densities of lipid, acyl chain, phosphate, choline nitrogen, chloride, and sodium. The results match the non-proteinaceous densities of cryo-EM maps in both cross-section view and axial view. To further confirm that the extra densities are from lipids, the authors modeled POPC/POPA molecule into the well-defined densities of each polymorph, as in Fig. 4, which may indicate the conformation of POPC/POPA molecule. Moreover, the detailed structural analysis about the interaction between α-syn fibrils and the docked POPC/POPA is absent. Additional interaction analysis may provide a clear view of how the micelle-like lipids pack on the fibril surface.
2. It seems that the structural model coordinates and the cryo-EM maps have not been submitted to PDB or EMDB. I strongly suggest the authors upload the files to these two databases and provide full wwPDB validation reports.
3. Whether POPC/POPA vesicles affect the fibrillation kinetics of α-syn? The authors might need to perform ThT fluorescence assay to monitor the α-syn fibrillation kinetics in the presence of lipids.
4. The authors might need to compare the L1 fibril fold with previously reported different α-syn folds, and discuss what's the novel structural feature of this fold.
5. The distinct packing pattern of protofilaments in L2B and L3A fibrils is interesting and features a novel protofilamental packing symmetry. How did the authors determine the handedness of these fibrils? Atomic force microscope can be used to characterize the handedness of fibril twist. For high resolution maps, densities for the carbonyl oxygen atoms may also help to confirm the handedness.
6. The authors need to clarify how the relative population of each lipid-α-syn fibril polymorphs (Extended Data Fig. 1g) is determined.
7. As for the statement "In the L1B fibril, both protofilaments are related by an approximate 21 screw symmetry and the protofilaments are tilted by ~37° to each other.", how is the tilt angle measured?

Minor concerns:
1. As for L1C, "ionic interactions between residues K45 and E46 form the inter-protofilament interface" should be "K43, K45 and E57";
2. Twist angle of L1A in Figure 1b should be consistent with the number in Extended Data Table 4;
3. Initial model used for model building of L3A should be 6UFR;
4. The tables cited in the main text is not in a right order.

Reviewer #2 (Remarks to the Author):

The manuscript describes cryo-EM structures of six α-synuclein fibril polymorphs in complex with lipids. The phospholipids are suggested to induced (some) new morphologies of the fibrils and to bind to cavities within them. The authors suggest that the structures support a mechanism of co-aggregation of lipids with fibril, and to fibril-induced lipid extraction, leading to cell toxicity and pathology via disruption of intracellular vesicles.

The "big question" here is whether the lipids really induce specific conformations that are relevant to membrane interactions or rather are just "additional polymorphs" of a-syn that are induced by different conditions or a part of an inherent population mix. I think it is impossible to answer this question with current tools. There are few residues that were correlated with lipid interactions, but this is a very limited information and support. The most convincing evidence is the presence of lipids in the central cavity of L2A that might mediate the interaction between the protofilaments. Having said that, the L2A protofilament arrangement was observed without lipids, then yet the intertwining of the protofilaments might be lipid induced and relevant. Really impossible to tell. I agree that it is tempting to suggest that the structures support a proposed lipid extraction mechanism and co-aggregation of lipids with fibrils.

1. Another conceptual question is the colloidal state of the lipids which encounter the protein/fibres. Is it in the presence of vesicles or micelles (probably affected by the sonication/incubation)? Or some other type of colloidal system?
This might be relevant in case the interaction / state of the lipids after sonication is different in comparison to a vesicular system which resembles more physiological condition. Why didn't you use intact vesicles?

Technical comments:
2. Fig 3 – "In a+d, the arrows highlight non-fibrillar densities" – should it be a-f? I think there is a mix-up in the colours of the map in the figure legend.
3. The residues that were identified by ssNMR to bind to the PLs are not named explicitly except from within the image itself (3 hydrophobic residues? – what about the headgroups?).
4. Fig 3d,e – points to L1B and it is refer in the text discussing K6, K21, and E20 - but these are not shown.
5. Fig 3f – L1C fibril - K43, K45, and E57 should be shown in closeness to the Cl ion as discussed in the text.
6. Fig 3h - L2A - it is impossible to appreciate the real distance between the lysines and the Cl ions in this figure. "where Cl- ions colocalize with head groups at the interface between K43 and K45 (Fig. 3a,i,j)" – one cannot see it clearly in 3i,j and definitely not in 3a. zoom-in is needed.
7. Segments 35-EGVLYV-40 and 34-KEGVLYVGSK-45 should be indicated in the figures. Also a zoom-in of Y39.
8. Please indicate the FSC=0.143 resolution in Extended Data Fig. 2 (crossing lines or something similar).
9. I am confused by the 2.37A helical rise of L1B. In the FSC there is a peak at ~4.7A which is similar to the other polymorphs.
10. In page 6 line 4 is stated:" The conversion of the SUVs used for the preparation of the lipidic fibrils to such small lipid aggregates upon fibril formation was confirmed by 31P ssNMR", so it means that the SUVs were used as initial system? Is it the same lipid state as used for the cryo-EM?
11. Why are the PDB reports "*Not For Manuscript Review? I have never seen this statement. There are many clashes, but I think mostly of hydrogens, so it is fine. Anyway, the resolution seems to be good enough to avoid clashes.

Reviewer #3 (Remarks to the Author):

The authors of the study present 6 new cryo-electron microscopy α-synuclein fibril structures. They also support their experimental work with MD simulations. The study is well-structured, up-to-date and original, and provides new insigts on lipid- α-synuclein fibril interactions that could guide future therapeutic applications for PD. However, authors should address the following

questions before work is accepted

- Although the authors gave a reference, how many ns did it reach thermalization and density adaptation in MD simulations? this time period should be included in the manuscript. Also, is it possible to embedded a visual proof of these metrics on the supporting information?
- In which statistical ensemble did the authors perform their equilibration simulations? this must be stated in the manuscript.
- It was interesting that the MD replicas were produced at the start of the NPT production simulations. Could the replicas have been produced at the start of the balancing simulations? Can the authors review this situation? Also, how were the initial velocities for these replicas randomly determined? Were they produced based on any physical function?
-The authors say that after 100 ns, the simulations convergence. Can they justify this situation with various visual metrics and put them in supporting information?
-In the simulation video, it looks like position constraints have been applied to the fibrils. If so, the authors should definitely state this situation in the manuscript along with their reasons.

Reviewer #4 (Remarks to the Author):

The authors present structures of alpha-synuclein fibrils prepared from in vitro incubation with phospholipids. This is highly significant work because it presents the first direct structural evidence of lipid interactions with synuclein fibrils and the structures are good quality.

Some drawbacks of the study are that the lipid to protein ratios are unusually low and there are large differences among the various structures observed, so it is not clear whether these actually represent situations observed physiologically. This criticism, however, is true for most alpha-synuclein structural studies, so it is not a fatal flaw.

The structures are well described and complementary MD simulations and solid state NMR studies support the overall impact of the work.

The validation reports indicate that they are not intended for submission to manuscripts so this seems awkward.

RESPONSE TO REVIEWERS' COMMENTS

We thank the four reviewers for the evaluation of our manuscript and for their many helpful comments and suggestions for improvements. In the following, the reviewer comments are in *italics* and our responses start with "**A:**". Although not all text changes are reproduced in this response letter, selected parts of the revised manuscript text are highlighted in green. We believe that, thanks to the reviewer input, the manuscript has greatly improved.

Reviewer #1 (Remarks to the Author):

Frieg et al. present cryo-EM analysis of phospholipid-induced α-synuclein (lipid-α-syn) fibril structures, and reveal the structural basis of the interaction between lipid and α-syn in fibrillar form from the additional cryo-EM densities of on lipid-α-syn fibril together with MD simulations and ssNMR data. The authors determine six lipid-α-syn fibril complex structures. Interestingly, three L1 fibrils possess a novel protofilament fold type, which expands the structural knowledge on the structural polymorphism of α-syn amyloid fibril. L2 and L3 feature previously knownα-syn fold in fibril structures, but with distinct protofilamental arrangement. Moreover, the MD simulations of lipid diffusion in the presence ofα-syn fibril structure suggest a micelle-like lipid arrangements at the fibril surface and the central cavity, which matches the cryo-EM densities well. By further performing ssNMR, the authors assign the fibril-lipid interactions for each fibril polymorph. Both lipid and α-syn fibrils are enriched in Lewy bodies in the patients' brains of Parkinson's disease. Elucidating lipid-α-syn fibril interaction is important to understanding the molecular basis of α-syn pathological aggregation and Lewy body formation in PD. Thus, this work is timely and important to the field. Overall, the results are well presented in a logic format, and the complex structural models are cross-validated by different biophysical and computational methods. To strengthen this work, the authors may need to address my concerns listed below.

Major concerns:

1. The authors perform MD simulations for phospholipid diffusion and show probability densities of lipid, acyl chain, phosphate, choline nitrogen, chloride, and sodium. The results match the non-proteinaceous densities of cryo-EM maps in both cross-section view and axial view. To further confirm that the extra densities are from lipids, the authors modeled POPC/POPA molecule into the well-defined densities of each polymorph, as in Fig. 4, which may indicate the conformation of POPC/POPA molecule. Moreover, the detailed structural analysis about the interaction between α-syn fibrils and the docked POPC/POPA is absent. Additional interaction analysis may provide a clear view of how the micelle-like lipids pack on the fibril surface.

A: Following the reviewer's suggestion for a detailed structural analysis of αSyn-POPA/POPC interactions, we analyzed the MD trajectories towards residue-wise interactions not only with POPA and POPC, but also including Na^+ and Cl^- atoms. To do so, we measured the minimal distance between any non-hydrogen atom of every amino acid of five layers from the center of each protofilament to (i) the phosphate group of the phospholipids, (ii) the quaternary choline group

of the phospholipids, (iii) any carbon atom of the acyl chains of the phospholipids, (iv) any Na^+, and (v) any Cl^- ion. An interaction was present, if the distance was smaller than 5 Å. These interactions are normalized by the total number of frames, so that a value of 1.0 means "interaction always present", whereas a value of 0.0 means "interaction not existent". We considered an amino acid as "interacting", if the interaction is present in at least 50% (value 0.5) of all conformations and "strongly interacting" if the interaction is present in at least 75% (value 0.75) of all conformations. The results are shown in the new Fig. 4 (p. 15).

In addition, we extended the description and interpretation of the MD simulation data in the revised manuscript, which reads (pp. 6): "The patterns of lipid interactions per residue repeated in all *L1* fibrils suggest that lipid-mediated intramolecular interactions may be necessary for the novel *L1* folding. For all *L1* lipids, the predominantly hydrophobic segments $_1$MDVFM$_5$, $_{36}$GVLYV$_{40}$, $_{69}$AVVTGVTAVA$_{78}$, and $_{85}$AGSIAAATGFV$_{95}$ are in contact with the lipidic acyl chains. At the same time, the adjacent polar residues K6, E20, K21, K32, E35, N79, K80, and S87 interact with the lipidic head groups (**Fig. 4**). Hence, hydrophobic areas on the fibril surface are, at least partially, covered with phospholipids. **Fig. 5** shows a POPC molecule modeled into the most well-defined non-proteinaceous densities at the fibril surface.

The central cavity in the *L1B* fibril is occupied by lipids, with their head groups bridging interactions between K6, K21, E20, and E35, while their acyl chains form hydrophobic interactions with M1, V2, M5, G36, L38, and V40 bridging across the protofilament interface (**Fig. 3d, e, Fig. 4**). The MD simulations revealed that the *L1B* cavity is occupied by chloride ions (Cl^-), which are complexed by the positively charged residues K21 and K23. For the *L1C* fibril, also revealed a high probability for Cl^- ions in the hydrophilic interface involving residues K43, K45, and E57 is found (**Fig. 3f,g, Fig. 4**).

A striking feature of the *L2A* fibril is the bridging of lipid molecules that span the ~20 Å gap between the protofilaments. The simulations revealed that lipids interact with the segment $_{33}$TKEGVLYVGSKTK$_{45}$, bridging the gap between the protofilaments. In detail, the acyl chains bind to Y39, V40, and G41, which form a small hydrophobic patch at the fibril surface (**Fig. 4**). Additionally, the lipidic head groups interact with K43 and K45 on one protofilament and with K34 on the neighboring protofilament (**Fig. 4**). The head group densities of these lipids partially overlap with densities for Cl^- (**Fig. 3h**) and the per-residue analysis confirmed that K34, K43, and K45 also interact with Cl^- (**Fig. 4**). Hence, the negatively charged phosphate groups and the Cl^- ions together form the bridge between K34 and K43 in the individual protofilaments by forming a well-ordered interaction network.

Although the *L2* and *L3* folds appear reminiscent of reported structures[26,27], fibril-lipid interactions favor novel quaternary protofilament arrangements. In the *L2A* fibril, lipid-mediated interactions seem to be essential as they connect the neighboring protofilaments. Lipid-mediated interactions might also be responsible for the protofilaments pointing in opposite directions in the *L2B* and *L3A* fibrils, as in this configuration, two mirrored $_{34}$KEGVLYVGSK$_{43}$ segments from both protofilaments are in contact with the same phospholipid micelle (**Fig. 3i, j**). Again, the acyl chains bind to Y39, V40, and G41, the head groups interact with K34, K43, and K45 on both protofilaments, and Cl^- ions colocalize with head groups at the interface between K43 and K45 (**Fig. 4**)."

2. It seems that the structural model coordinates and the cryo-EM maps have not been submitted to PDB or EMDB. I strongly suggest the authors upload the files to these two databases and provide full wwPDB validation reports.

A: For the revision, we now uploaded the atomic models and the cryo-EM maps to PDB and EMDB, respectively. The accession codes are reported in the **Extended Data Tab. 1** on page 47. Please also find a summary below.

Lipid-induced PM	*L1A*	*L1B*	*L1C*	*L2A*	*L2B*	*L3A*
PDB-ID	8ADU	8ADV	8ADW	8A4L	8ADS	8AEX
EMDB-ID	15370	15371	15372	15148	15369	15388

3. Whether POPC/POPA vesicles affect the fibrillation kinetics of α-syn? The authors might need to perform ThT fluorescence assay to monitor the α-syn fibrillation kinetics in the presence of lipids.

A: The influence of POPC/POPA vesicles has been studied before in the same L/P range as presented here and showed an acceleration of α-synuclein aggregation (Jiang, de Messieres, and Lee, *J. Am. Chem. Soc.*, 2013). This was also reported for a multitude of other negatively charged phospholipids and our results show a similar trend. We added representative curves as Extended Data Fig. 1b (p. 27).
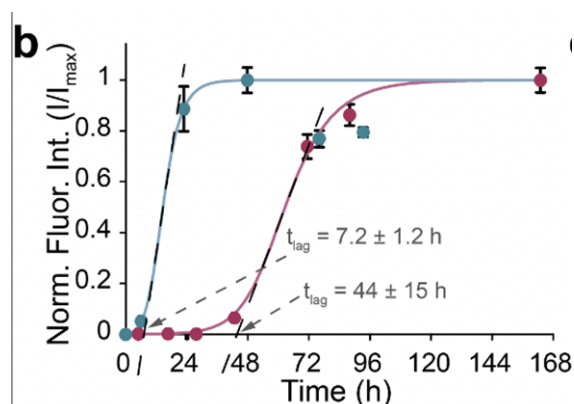
Extended Data Fig. 1b: Representative curves of normalized ThT fluorescence (I/I_{max}) following the aggregation kinetics of αSyn in the presence (blue) and absence (magenta) of vesicles of POPA and POPC (1:1) under PMCA conditions. Curves were obtained by fitting the data to an unseeded secondary nucleation model using Amylofit[65] (www.amylofit.ch.cam.ac.uk/). Lag-times t_{lag} were determined as the intersection of the x-axis and a linear function fitted to the steepest part of the curve

4. The authors might need to compare the L1 fibril fold with previously reported different α-syn folds, and discuss what's the novel structural feature of this fold.

A: Following the reviewer's suggestion, we extended the description of the novel *L1* fold and compare the L1 fold to previously determined structures. Therefore, we added **Extended Data Fig. 4** in the revised version of the manuscript. The comparison starts on p. 4 at line 23 and reads: "The lipidic *L1* fold reveals minor similarities to previously resolved structures of αSyn in the absence of phospholipids (**Extended Data Fig. 4a**). In detail, only the fold of the *L1* segment V52 - T72 is found in the protofilament fold of wild type and Y39 phosphorylated αSyn (**Extended Data Fig. 4b, c**). This discrepancy with previously resolved structures is probably related to the presence of phospholipids during αSyn aggregation. While the previously determined structures are characterized by a predominantly hydrophobic core, in the *L1* fold a surprisingly large number of hydrophobic residues are found on the surface (**Extended Data Fig. 4d**). However, these "solvent-exposed" areas are decorated with non-proteinaceous densities (**Fig. 1f-h**), corresponding to surface-bound phospholipids (for details, see below). Hence, the phospholipids may shield, at least to some extent, the hydrophobic amino acids on the fibril surface from direct interactions with water during αSyn aggregation, which then leads to the lipid-mediated *L1* fold."

5. The distinct packing pattern of protofilaments in L2B and L3A fibrils is interesting and features a novel protofilamental packing symmetry. How did the authors determine the handedness of these fibrils? Atomic force microscope can be used to characterize the handedness of fibril twist. For high resolution maps, densities for the carbonyl oxygen atoms may also help to confirm the handedness.

A: We did not perform any additional experiment to investigate the handedness of the fibrils. However, *for all fibrils we found regions in the structure where the local resolution is sufficient to identify the orientation of the backbone carbonyl groups, and with this all fibrils were found to have a left-handed twist.* We have added this sentence to the Methods section.

6. The authors need to clarify how the relative population of each lipid-α-syn fibril polymorphs (Extended Data Fig. 1g) is determined.

A: We added an additional section (*Determination of the relative population of each fibril polymorph*) to the Methods part, which reads (p. 20): "In the cases of *L1A*, *L1B*, *L1C*, and *L2A* fibrils, the population relative to the total number of extracted helical segments was calculated based on the number of helical segments after the successful separation by 2D classification. As to *L2B* and *L3A*, on the other hand, we used the number of helical segments after successful separation by 3D classification."

7. As for the statement "In the L1B fibril, both protofilaments are related by an approximate 2₁ screw symmetry and the protofilaments are tilted by ~37° to each other.", how is the tilt angle measured?

A: To estimate the tilt angle between the protofilaments, we measure the dihedral angle described by the Cα atoms of M1-V40-M1'-V40' of two opposite protein chains. In the revised manuscript, please find the novel Extended Data Fig. 5 (p. 33) visualizing the tilted orientation of the protofilaments in *L1B*. For comparison, we also show *L1C* with an almost planar orientation of the protofilaments.

Minor concerns:

1. As for L1C, "ionic interactions between residues K45 and E46 form the inter-protofilament interface" should be "K43, K45 and E57";

2. Twist angle of L1A in Figure 1b should be consistent with the number in Extended Data Table

3. Initial model used for model building of L3A should be 6UFR;

4. The tables cited in the main text is not in a right order.

A: We highly appreciate the careful reading. All concerns have been addressed in the revised manuscript.

Reviewer #2 (Remarks to the Author):

The manuscript describes cryo-EM structures of six α-synuclein fibril polymorphs in complex with lipids. The phospholipids are suggested to induced (some) new morphologies of the fibrils and to bind to cavities within them. The authors suggest that the structures support a mechanism of co-aggregation of lipids with fibril, and to fibril-induced lipid extraction, leading to cell toxicity and pathology via disruption of intracellular vesicles.

The "big question" here is whether the lipids really induce specific conformations that are relevant to membrane interactions or rather are just "additional polymorphs" of a-syn that are induced by different conditions or a part of an inherent population mix. I think it is impossible to answer this question with current tools. There are few residues that were correlated with lipid interactions, but this is a very limited information and support. The most convincing evidence is the presence of lipids in the central cavity of L2A that might mediate the interaction between the protofilaments. Having said that, the L2A protofilament arrangement was observed without lipids, then yet the intertwining of the protofilaments might be lipid induced and relevant. Really impossible to tell. I agree that it is tempting to suggest that the structures support a proposed lipid extraction mechanism and co-aggregation of lipids with fibrils.

1. Another conceptual question is the colloidal state of the lipids which encounter the protein/fibres. Is it in the presence of vesicles or micelles (probably affected by the sonication/incubation)? Or some other type of colloidal system?

This might be relevant in case the interaction / state of the lipids after sonication is different in comparison to a vesicular system which resembles more physiological condition. Why didn't you use intact vesicles?

A: The main text did not make it obvious that we indeed started with intact small unilamellar vesicles (SUVs). We changed the text accordingly to avoid any confusion to the future reader. The new paragraph reads (p. 4, line 2): "*De novo* aggregation in the presence of small unilamellar vesicles (SUVs) at a 5:1 lipid to protein ratio was induced by sonication under protein misfolding cyclic amplification conditions and completed under gentle orbital shaking to elongate the fibrils[20]. SUVs consisted of a 1:1 mixture of 1-palmitoyl-2-oleoyl-sn-glycero-3-phosphate (POPA) and 1-palmitoyl-2-oleoyl-sn-glycero-3-phosphocholine (POPC) as a simplification of negatively charged synaptic vesicles[21] to recapitulate the established binding of monomeric αSyn to lipids via its N-terminus[22,23]. In agreement with previous studies we observed significantly reduced lag-times in the presence of these phospholipids[24]."

Technical comments:

2. Fig 3 – "In a+d, the arrows highlight non-fibrillar densities" – should it be a-f? I think there is a mix-up in the colours of the map in the figure legend.

A: We appreciate the careful reading and fixed the mismatch in the revised manuscript.

3. The residues that were identified by ssNMR to bind to the PLs are not named explicitly except from within the image itself (3 hydrophobic residues? – what about the headgroups?).

A: (Please see the combined answer on comment #7)

4. Fig 3d,e – points to L1B and it is refer in the text discussing K6, K21, and E20 - but these are not shown.

A: (Please see the combined answer on comment #7)

5. Fig 3f – L1C fibril - K43, K45, and E57 should be shown in closeness to the Cl ion as discussed in the text.

A: (Please see the combined answer on comment #7)

6. Fig 3h - L2A - it is impossible to appreciate the real distance between the lysines and the Cl ions in this figure. "where Cl- ions colocalize with head groups at the interface between K43 and K45 (Fig. 3a,i,j)" – one cannot see it clearly in 3i,j and definitely not in 3a. zoom-in is needed.

A: (Please see the combined answer on comment #7)

7. Segments 35-EGVLYV-40 and 34-KEGVLYVGSK-45 should be indicated in the figures. Also a zoom-in of Y39.

A: In the revised manuscript, we now include a detailed structural analysis of the interactions between αSyn and POPA, POPC, Na$^+$, and Cl$^-$ throughout the MD simulations. To do so, we measured the minimal distance between any non-hydrogen atom of every amino acid of the central five layers of each protofilament to (i) the phosphate group of the phospholipids, (ii) the quaternary choline group of the phospholipids, (iii) any carbon atom of the acyl chains of the phospholipids, (iv) any Na$^+$, and (v) any Cl$^-$ ion. An interaction was present, if the distance was smaller 5 Å. These interactions are normalized by the total number of frames, so that a value of 1.0 means "interaction always present", whereas a value of 0.0 means "interaction never existent". We considered an amino acid as "interacting", if the interaction is present in at least 50% (value 0.5) off all conformations and "strongly interacting" if the interaction is present in at least 75% (value 0.75) off all conformations. The results are shown in the new Fig. 4 (p. 15).

In addition, we extended the description and interpretation of the MD simulation data in the revised manuscript, which reads (pp. 6): "The patterns of lipid interactions per residue repeated in all *L1* fibrils suggest that lipid-mediated intramolecular interactions may be necessary for the novel *L1* folding. For all *L1* lipids, the predominantly hydrophobic segments $_1$MDVFM$_5$, $_{36}$GVLYV$_{40}$, $_{69}$AVVTGVTAVA$_{78}$, and $_{85}$AGSIAAATGFV$_{95}$ are in contact with the lipidic acyl chains. At the same time, the adjacent polar residues K6, E20, K21, K32, E35, N79, K80, and S87 interact with the lipidic head groups (**Fig. 4**). Hence, hydrophobic areas on the fibril surface are, at least partially,

covered with phospholipids. **Fig. 5** shows a POPC molecule modeled into the most well-defined non-proteinaceous densities at the fibril surface.

The central cavity in the *L1B* fibril is occupied by lipids, with their head groups bridging interactions between K6, K21, E20, and E35, while their acyl chains form hydrophobic interactions with M1, V2, M5, G36, L38, and V40 bridging across the protofilament interface (**Fig. 3d, e, Fig. 4**). The MD simulations revealed that the *L1B* cavity is occupied by chloride ions (Cl⁻), which are complexed by the positively charged residues K21 and K23. For the *L1C* fibril, also revealed a high probability for Cl⁻ ions in the hydrophilic interface involving residues K43, K45, and E57 is found (**Fig. 3f,g, Fig. 4**).

A striking feature of the *L2A* fibril is the bridging of lipid molecules that span the ~20 Å gap between the protofilaments. The simulations revealed that lipids interact with the segment ₃₃TKEGVLYVGSKTK₄₅, bridging the gap between the protofilaments. In detail, the acyl chains bind to Y39, V40, and G41, which form a small hydrophobic patch at the fibril surface (**Fig. 4**). Additionally, the lipidic head groups interact with K43 and K45 on one protofilament and with K34 on the neighboring protofilament (**Fig. 4**). The head group densities of these lipids partially overlap with densities for Cl⁻ (**Fig. 3h**) and the per-residue analysis confirmed that K34, K43, and K45 also interact with Cl⁻ (**Fig. 4**). Hence, the negatively charged phosphate groups and the Cl⁻ ions together form the bridge between K34 and K43 in the individual protofilaments by forming a well-ordered interaction network.

Although the *L2* and *L3* folds appear reminiscent of reported structures[26,27], fibril-lipid interactions favor novel quaternary protofilament arrangements. In the *L2A* fibril, lipid-mediated interactions seem to be essential as they connect the neighboring protofilaments. Lipid-mediated interactions might also be responsible for the protofilaments pointing in opposite directions in the *L2B* and *L3A* fibrils, as in this configuration, two mirrored ₃₄KEGVLYVGSK₄₃ segments from both protofilaments are in contact with the same phospholipid micelle (**Fig. 3i, j**). Again, the acyl chains bind to Y39, V40, and G41, the head groups interact with K34, K43, and K45 on both protofilaments, and Cl⁻ ions colocalize with head groups at the interface between K43 and K45 (**Fig. 4**)."

In contrast to the reviewer's suggestion to show a structure from the MD ensemble with zoom-in onto the areas of interest, this approach provides an even more detailed picture about the lipid interactions, as it includes the ensemble information and not only one snapshot. We assume that such an analysis will also help the future reader to get a clear picture about the interactions of αSyn, lipids, and ions.

8. Please indicate the FSC=0.143 resolution in Extended Data Fig. 2 (crossing lines or something similar).

A: In the revised manuscript, we now show FSC=0.143 as gray line (see Extended Data Fig. 3 on p. 30).

9. I am confused by the 2.37A helical rise of L1B. In the FSC there is a peak at ~4.7A which is similar to the other polymorphs.

A: In the L1B fibril both protofilaments are related by an approximate 2_1 screw symmetry, leading to a staggered arrangement of the of the protofilaments relative to each other, which is also visualized in the close-up view in Fig. 1c. Still, within one protofilament the stacked αSyn peptides are separated by 4.74 Å. However, as the helical rise describes the spatial displacement of two asymmetric units along the helical axis, the rise between two staggered protofilaments yields 2.37 Å.

To avoid any confusion to the future reader, we modified Fig. 1c and now also show the rise per protofilament (= 4.74 Å) and the rise between two staggered protofilaments (= 2.37 Å).

10. In page 6 line 4 is stated:'' The conversion of the SUVs used for the preparation of the lipidic fibrils to such small lipid aggregates upon fibril formation was confirmed by 31P ssNMR'', so it means that the SUVs were used as initial system? Is it the same lipid state as used for the cryo-EM?

A: Yes, SUVs were used to during αSyn aggregation. As stated above (please see comment 1), we now explicitly mention the SUVs in the main text.

*11. Why are the PDB reports "*Not For Manuscript Review? I have never seen this statement. There are many clashes, but I think mostly of hydrogens, so it is fine. Anyway, the resolution seems to be good enough to avoid clashes.*

A: We have now deposited the atomic models and the cryo-EM maps to PDB and EMDB, respectively. The accession codes are reported in the **Extended Data Tab. 1** on page 47. Please also find a summary below. The number of clashes is slightly higher than average observed for EM structures of similar resolution, however we think the number of clashes is still in an acceptable range.

Lipid-induced PM	*L1A*	*L1B*	*L1C*	*L2A*	*L2B*	*L3A*
PDB-ID	8ADU	8ADV	8ADW	8A4L	8ADS	8AEX
EMDB-ID	15370	15371	15372	15148	15369	15388

Reviewer #3 (Remarks to the Author):

The authors of the study present 6 new cryo-electron microscopy α-synuclein fibril structures. They also support their experimental work with MD simulations. The study is well-structured, up-to-date and original, and provides new insigts on lipid- α-synuclein fibril interactions that could guide future therapeutic applications for PD. However, authors should address the following questions before work is accepted

- Although the authors gave a reference, how many ns did it reach thermalization and density adaptation in MD simulations? this time period should be included in the manuscript. Also, is it possible to embedded a visual proof of these metrics on the supporting information?

A: (please see next comment)

- In which statistical ensemble did the authors perform their equilibration simulations? this must be stated in the manuscript.

A: (please see next comment)

- It was interesting that the MD replicas were produced at the start of the NPT production simulations. Could the replicas have been produced at the start of the balancing simulations? Can the authors review this situation? Also, how were the initial velocities for these replicas randomly determined? Were they produced based on any physical function?

A: Following the reviewers suggestions, we now show the thermalization and density adaptation data in the new **Extended Data Fig. 9** (p. 42). Additionally, the figure caption also includes a description of the simulation procedure. The new caption (starting on p. 43) reads: "Time series of the temperature (left panels) and density (right panels) over 0.6 ns of MD simulations for *L1A* (**a**), *L1B* (**b**), *L1C* (**c**), *L2A* (**d**), *L2B* (**e**), and *L3A* (**f**). The MD simulation procedure[58] started by heating the systems from 0 K to 100 K in a canonical (NVT) MD simulation of 50 ps length. Afterward, the temperature was raised from 100 K to 300 K during 50 ps of isobaric-isothermal (NPT) MD. Subsequently, the density was gently adjusted to 1 g/ml during 200 ps of NPT-MD. During the heating and density adaptation steps, positional restraints of 1 kcal·mol^{-1}·Å^{-2} were applied to all backbone and lipidic phosphate atoms. These harmonic positional restraints were removed from the lipidic phosphate atoms by gradually decreasing the force constant from 1 to 0 kcal·mol^{-1}·Å^{-2} in six NPT-MD runs of 50 ps length each. From here, we (re-)started eight independent NPT production simulations at 300 K and 1 bar for 1 µs each, in that new velocities were assigned from Maxwell-Boltzmann distribution. Importantly, we restrained the backbone to the initial atomic coordinates throughout production simulations while all other atoms were allowed to move freely."

-The authors say that after 100 ns, the simulations convergence. Can they justify this situation with various visual metrics and put them in supporting information?

A: We more specifically only claimed that the distribution of lipids converge after 100 ns, we wrote: "*Thereby, we observed only minimal changes when extending the analysis time from 0.9 µs ns to 1.0 µs, such that we assumed converged distributions of the lipid molecules.*". However, we agree with the reviewer that some visual proof may increase the understanding and in the revised

manuscript we now show the progression of the density grids throughout one replica simulation for all six fibril structure in the new <mark>Extended Data Fig. 11</mark> (p. 45)**.** Although we decided to focus on the distribution of the lipids and do not show the density grids of ions for clarity purposes, the <mark>Extended Data Fig. 11</mark> visualizes that, first, major changes in lipid distribution appear on the first 0.3 µs, second, the changes in the lipid distribution are minimal when extending the analysis time from 0.6 µs to 0.7 µs, and, finally, the changes in the lipid distribution are neglectable when extending the analysis time from 0.9 µs to 1.0 µs. Hence, we assumed converged distributions of the lipid molecules.

-In the simulation video, it looks like position constraints have been applied to the fibrils. If so, the authors should definitely state this situation in the manuscript along with their reasons.

A: The fibril's backbone was restraint to the initial coordinates and we provided this information in the original manuscript in the Methods section: "*Importantly, we restrained the backbone to the initial atomic coordinates. However, all other molecules, including POPC and POPA, were allowed to diffuse freely and we did not apply any artificial guiding force.*". As suggested, we extended this section by a short explanation for our reason, including the novel <mark>Extended Data Fig. 10</mark> (p. 44), which shows RMSD plots of the fibril structures after 1 µs MD simulations without lipids and without positional restraints. We have to restrain the backbone because the fibrils are not stable without the proper converged lipid distribution around the fibril, which was not present at the beginning of the simulations. The <mark>Extended Data Fig. 10</mark> visualizes that the quaternary structures of the models are not stable without positional restraints.

Reviewer #4 (Remarks to the Author):

The authors present structures of alpha-synuclein fibrils prepared from in vitro incubation with phospholipids. This is highly significant work because it presents the first direct structural evidence of lipid interactions with synuclein fibrils and the structures are good quality.

Some drawbacks of the study are that the lipid to protein ratios are unusually low and there are large differences among the various structures observed, so it is not clear whether these actually represent situations observed physiologically. This criticism, however, is true for most alpha-synuclein structural studies, so it is not a fatal flaw.

The structures are well described and complementary MD simulations and solid state NMR studies support the overall impact of the work.

The validation reports indicate that they are not intended for submission to manuscripts so this seems awkward.

A: For resubmission, we uploaded the atomic models and the cryo-EM maps to PDB and EMDB, respectively, including final validation reports. The accession codes are reported in the **Extended Data Tab. 1** on page 47. Please also find a summary below.

Lipid-induced PM	*L1A*	*L1B*	*L1C*	*L2A*	*L2B*	*L3A*
PDB-ID	8ADU	8ADV	8ADW	8A4L	8ADS	8AEX
EMDB-ID	15370	15371	15372	15148	15369	15388

REVIEWERS' COMMENTS

Reviewer #1 (Remarks to the Author):

The authors addressed my concerns with satisfaction. I support publication of this work in NC.

Reviewer #2 (Remarks to the Author):

The authors have satisfactorily addressed my comments.

Reviewer #3 (Remarks to the Author):

The authors have made significant changes as per suggestions and have increased the quality of work and readability. I think manuscript can be considered for the publication.

nature portfolio

Corresponding author(s): G.F.Schröder and C.Griesinger

Last updated by author(s): Oct 10, 2022

Reporting Summary

Nature Portfolio wishes to improve the reproducibility of the work that we publish. This form provides structure for consistency and transparency in reporting. For further information on Nature Portfolio policies, see our Editorial Policies and the Editorial Policy Checklist.

Statistics

For all statistical analyses, confirm that the following items are present in the figure legend, table legend, main text, or Methods section.

n/a	Confirmed	
☐	☒	The exact sample size (*n*) for each experimental group/condition, given as a discrete number and unit of measurement
☐	☒	A statement on whether measurements were taken from distinct samples or whether the same sample was measured repeatedly
☒	☐	The statistical test(s) used AND whether they are one- or two-sided *Only common tests should be described solely by name; describe more complex techniques in the Methods section.*
☒	☐	A description of all covariates tested
☒	☐	A description of any assumptions or corrections, such as tests of normality and adjustment for multiple comparisons
☐	☒	A full description of the statistical parameters including central tendency (e.g. means) or other basic estimates (e.g. regression coefficient) AND variation (e.g. standard deviation) or associated estimates of uncertainty (e.g. confidence intervals)
☒	☐	For null hypothesis testing, the test statistic (e.g. F, t, r) with confidence intervals, effect sizes, degrees of freedom and P value noted *Give P values as exact values whenever suitable.*
☒	☐	For Bayesian analysis, information on the choice of priors and Markov chain Monte Carlo settings
☒	☐	For hierarchical and complex designs, identification of the appropriate level for tests and full reporting of outcomes
☒	☐	Estimates of effect sizes (e.g. Cohen's *d*, Pearson's *r*), indicating how they were calculated

Our web collection on statistics for biologists contains articles on many of the points above.

Software and code

Policy information about availability of computer code

Data collection	TopSpin(v3.5.7), SerialEM(v4.0)
Data analysis	RELION (v3.1), CTFFIND (v4.1), COOT (v0.9), Chimera (v1.8.1), PHENIX (v1.19.2), PACKMOL (v20.3.5), Amber (v20)

For manuscripts utilizing custom algorithms or software that are central to the research but not yet described in published literature, software must be made available to editors and reviewers. We strongly encourage code deposition in a community repository (e.g. GitHub). See the Nature Portfolio guidelines for submitting code & software for further information.

Data

Policy information about availability of data

All manuscripts must include a data availability statement. This statement should provide the following information, where applicable:

- Accession codes, unique identifiers, or web links for publicly available datasets
- A description of any restrictions on data availability
- For clinical datasets or third party data, please ensure that the statement adheres to our policy

The cryo-EM maps have been deposited in the Electron Microscopy Data bank (EMDB) under the accession numbers EMD-15370 [https://www.ebi.ac.uk/pdbe/entry/emdb/EMD-15370] (L1A), EMD-15371 [https://www.ebi.ac.uk/pdbe/entry/emdb/EMD-15371] (L1B), EMD-15372 [https://www.ebi.ac.uk/pdbe/entry/emdb/EMD-15372] (L1C), EMD-15148 [https://www.ebi.ac.uk/pdbe/entry/emdb/EMD-15148] (L2A), EMD-15369 [https://www.ebi.ac.uk/pdbe/entry/emdb/EMD-15369] (L2B), and EMD-15388 [https://www.ebi.ac.uk/pdbe/entry/emdb/EMD-15388] (L3A). The corresponding atomic models have been deposited in the Protein Data Bank (PDB) under the accession numbers: 8ADU [https://doi.org/10.2210/pdb8ADU/pdb] (L1A), 8ADV [https://doi.org/10.2210/pdb8ADV/pdb] (L1B), 8ADW [https://doi.org/10.2210/pdb8ADW/pdb] (L1C), 8A4L [https://doi.org/ 10.2210/pdb8A4L/pdb] (L2A), 8ADS [https://doi.org/10.2210/pdb8ADS/pdb] (L2B), and 8AEX [https://doi.org/10.2210/pdb8AEX/pdb] (L3A). The data generated in this study are provided in the Source Data file. The data that support the findings of this study

are available from the corresponding author upon reasonable request.

Field-specific reporting

Please select the one below that is the best fit for your research. If you are not sure, read the appropriate sections before making your selection.

[×] Life sciences   [ ] Behavioural & social sciences   [ ] Ecological, evolutionary & environmental sciences

For a reference copy of the document with all sections, see nature.com/documents/nr-reporting-summary-flat.pdf

Life sciences study design

All studies must disclose on these points even when the disclosure is negative.

Sample size	We collected three datasets, one for each aggregation protocol. For the three datasets we collected 4.589, 4.324, and 4,542 micrographs, respectively. Number of datasets collected and the number of micrographs collected was limited by microscope measurement time and data processing time.
Data exclusions	Standard image classification procedures (Scheres, J. Struc. Biol. 180: 519-530, (2012)) were employed to select particle images with the goal to reach highest resolution reconstructions. Details of the number of selected images are given in Supplementary Table S1.
Replication	All determined fibril structures were replicated at least once from the three collected datasets. For the MD simulations, we performed eight replica simulations for each simulated polymorph.
Randomization	Randomization was not performed. We considered only three aggregation conditions. Randomization would therefore not remove any bias.
Blinding	Blinding was not performed, because the risk of bias in the results was considered negligible.

Reporting for specific materials, systems and methods

We require information from authors about some types of materials, experimental systems and methods used in many studies. Here, indicate whether each material, system or method listed is relevant to your study. If you are not sure if a list item applies to your research, read the appropriate section before selecting a response.

Materials & experimental systems

n/a	Involved in the study
[×] [ ]	Antibodies
[×] [ ]	Eukaryotic cell lines
[×] [ ]	Palaeontology and archaeology
[×] [ ]	Animals and other organisms
[×] [ ]	Human research participants
[×] [ ]	Clinical data
[×] [ ]	Dual use research of concern

Methods

n/a	Involved in the study
[×] [ ]	ChIP-seq
[×] [ ]	Flow cytometry
[×] [ ]	MRI-based neuroimaging